Int. J. Heat Mass Transfer. Vol. 15, pp. 789–800. Pergamon Press 1972. Printed in Great Britain

FINITE AMPLITUDE CONVECTION WITH LONGITUDINAL VORTICES IN PLANE POISEUILLE FLOW—THE EFFECT OF UNIFORM AXIAL TEMPERATURE GRADIENT

G. J. HWANG† and K. C. CHENG

Department of Mechanical Engineering, University of Alberta, Edmonton, Alberta, Canada

(*Received* 27 *May* 1971 *and in revised form* 18 *August* 1971)

Abstract—Finite amplitude convection with longitudinal vortex rolls for a steady hydrodynamically and thermally fully developed laminar forced flow between two infinite horizontal flat plates subjected to axially uniform wall heat flux is approached by a finite-difference solution using a combination of a boundary vorticity method and a line iterative relaxation technique. The governing equations with Boussinesq approximations are solved up to four times the critical value for the parameter ($PrReRa$). The onset of secondary flow in the form of longitudinal vortex rolls is indicated by a critical value $(PrReRa)^*$ which can be obtained by linear stability analysis with infinitesimal disturbance. The wave number in the post-critical flow regime is assumed to be that predicted by the linear stability analysis. The heat transfer mechanism is clarified by a detailed study of the field characteristics for flow and temperature using air ($Pr = 0{\cdot}7$) as an example. A series of photographs depicting the gradual development of the longitudinal vortex rolls for air is also presented. Flow and heat transfer results are presented for $Pr = 0{\cdot}1, 0{\cdot}7, 2, 10$ and 100. A study of the Prandtl number effect reveals that the effect of secondary flow on pressure-drop parameter fRe can be neglected for $Pr \geqslant 10$ and an asymptotic behavior for heat transfer results exists for $Pr \geqslant 2$ in the post-critical regime.

NOMENCLATURE

- a, dimensionless wave number in linear stability analysis, $2\pi h/\lambda$;
- f, Fanning friction factor;
- Gr, Grashof number, $g\beta\tau h^4/\nu^2$;
- g, gravitational acceleration;
- h, distance between two infinite parallel horizontal plates;
- M, number of divisions in both y' and z' directions;
- Nu, Nusselt number;
- P, pressure;
- p', disturbance pressure;
- Pr, Prandtl number, ν/κ;
- Ra, Rayleigh number, $PrGr$;
- Re, Reynolds number, $\bar{U}h/\nu$;
- Re_0, Reynolds number, $U_0h/2\nu$;
- T, temperature;
- U, V, W, velocity components in x', y' and z' directions;
- u, v, w, dimensionless velocity disturbances in x', y' and z' directions;
- u', v', w', velocity disturbances in x', y' and z' directions;
- x, y, z, dimensionless Cartesian coordinates;
- x', y', z', Cartesian coordinates.

Greek letters

- β, coefficient of thermal expansion;
- θ, dimensionless temperature disturbance;
- θ', temperature disturbance;
- κ, thermal diffusivity;
- λ, wave length of vortex rolls;

† Presently Visiting Associate Professor, Department of Mechanical Engineering, Cheng Kung University, Tainan, Taiwan, China.

μ, viscosity;
ν, kinematic viscosity;
ξ, dimensionless vorticity;
ξ', vorticity;
ρ, density;
τ, uniform axial temperature gradient for two plates, $\partial T/\partial X'$;
ϕ_u, basic velocity profile function;
ϕ_θ, basic temperature profile function;
ψ, dimensionless secondary flow stream function;
ψ', secondary flow stream function;
∇^2, dimensionless Laplacian operator, $\partial^2/\partial y^2 + \partial^2/\partial z^2$.

Subscript and superscript

*, critical value;
$^-$, mean value;
b, basic quantities in unperturbed state;
M, mixed mean value;
w, value at wall;
0, condition for pure forced convection or maximum quantity in unperturbed flow;
1, value at lower plate;
2, value at upper plate;
3, value obtained from overall balance.

1. INTRODUCTION

FOR HYDRODYNAMICALLY and thermally fully developed laminar forced convection between two infinite parallel plates with uniform wall heat flux, the Nusselt number based on the local difference between wall temperature and fluid bulk temperature is known to be 8·235 and the pressure-drop parameter fRe is 12 when the Reynolds number is based on channel height and mean velocity. Recently, it has been shown theoretically [1] and confirmed experimentally [2] that a secondary flow in the form of longitudinal vortices appears after the characteristic parameter $ReRa$ reaches a critical value for fully developed laminar forced convection between two infinite parallel horizontal plates subjected to uniform wall heat flux. For the present problem, only the fluid in the lower half of the horizontal parallel-plate channel is unstable because of an adverse temperature gradient and this leads to a thermal instability problem [1, 2]. It is evident that the theoretical predictions of $Nu = 8{\cdot}235$ and $fRe = 12$ for the no secondary flow case cannot be applied after the value for $ReRa$ reaches a critical value.

The onset and the subsequent formation of the longitudinal vortices in the post-critical flow regime are of considerable interest. Figure 1 presents a series of photographs taken from the exit of a horizontal rectangular channel with a cross section of 11 × 1 in. by injecting cigarette smoke into the heated main airflow. The flow visualization technique used is described in [2]. The gradual formation of the longitudinal vortex rolls is clearly demonstrated in Fig. 1 as the value for $ReRa$ is varied from $1{\cdot}47 \times 10^4$ to $4{\cdot}65 \times 10^4$. In addition to providing some insight into the development of the secondary flow pattern, the photographic results clearly indicate the extent of the free convection effect due to side walls.

It is noted that the thermal instability problem can be studied by employing linear stability analysis with infinitesimal disturbance while the flow and heat transfer problem in post-critical regime concerns disturbances with finite amplitude involving the nonlinear processes. The finite amplitude convection in a horizontal layer of fluid heated from below has been studied by many investigators. Since the literature on the Bénard–Rayleigh convection problem is too extensive to be reviewed here, only a brief review of the references closely related to the present study will be attempted.

Malkus and Veronis [3] proposed a finite amplitude method in an attempt to predict the heat transfer rates in a post-critical steady cellular flow regime for a layer of fluid heated uniformly from below and cooled from above. Stuart [4] described finite disturbances under subcritical and supercritical conditions by using an energy method and the shape of the amplitude functions obtained from the linearized

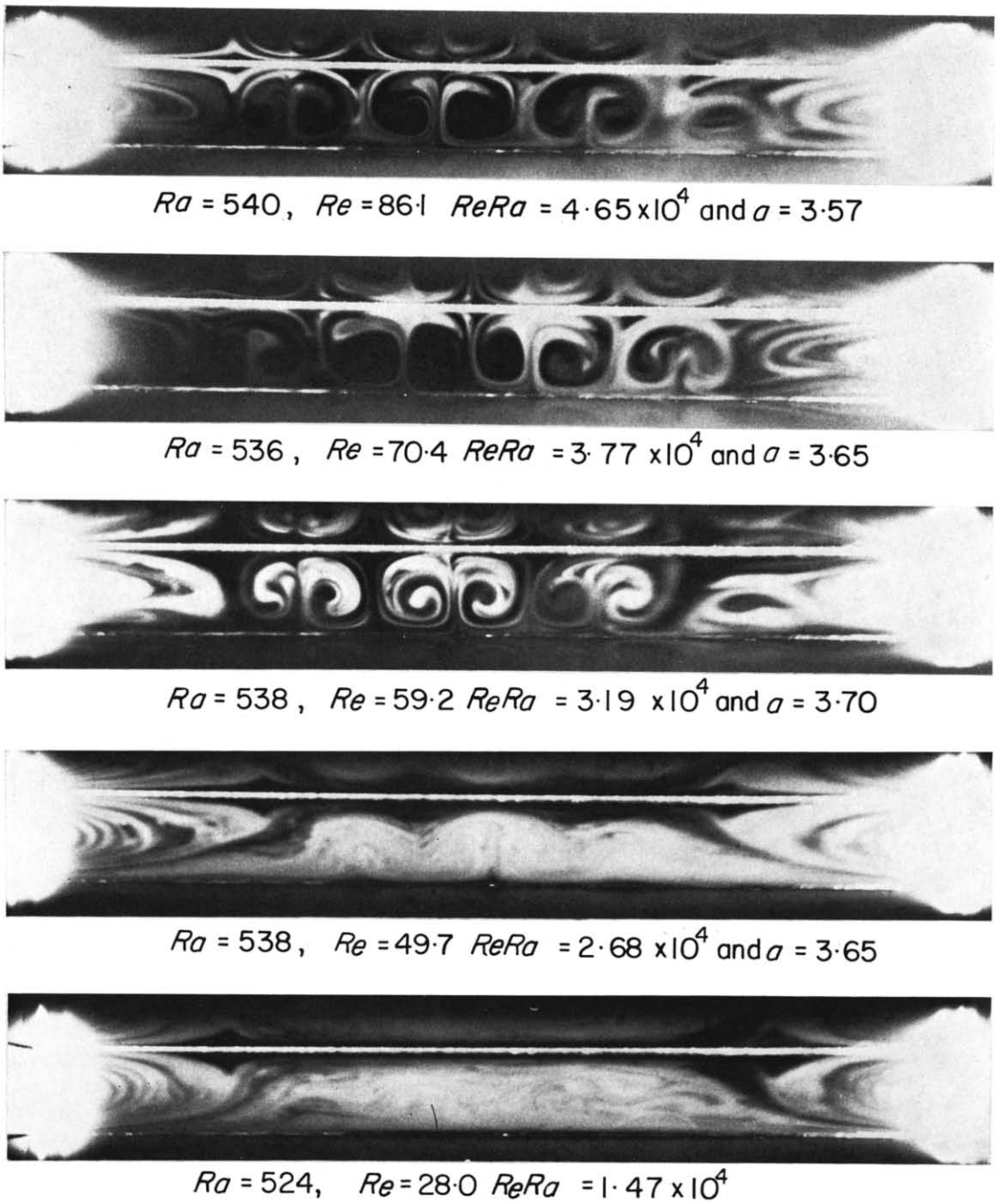

FIG. 1. Formation of longitudinal vortex rolls for air ($Pr = 0{\cdot}7$) in a horizontal rectangular channel (11 × 1in.) subjected to uniform wall heat flux with free convection effect near side walls.

H.M.

[facing page 790]

theory. Roberts [5] considered the nonlinear Bénard convection by using an approximate procedure. By employing the concept of local potential, Roberts [5] shows the behavior of the preferred wave number as a function of the Rayleigh number. The wave number is shown to vary from 0 to 1 per cent for Rayleigh number ranging from 1708 and 4000. However, the small variation of the wave number may not have significant effect on the heat transfer result. Both Fromm [6] and Plows [7] solved the Bénard convection problem by numerical methods using the wave number obtained from the linear stability theory.

Mori and Uchida [8] applied Stuart's approximate energy method for nonlinear mechanics of hydrodynamic stability [4] to fully developed laminar forced convection between two infinite horizontal flat plates where the lower plate is heated isothermally and the upper plate is cooled isothermally. For this problem, the critical Rayleigh number of 1708 marking the onset of thermal instability is known to be identical to that for the Bénard problem. It is noted that Stuart's method represents an approximation to a perturbation theory about the critical characteristic number and cannot be expected to be valid for a wide range of Rayleigh numbers above the critical value. Recently, Ogura and Yagihashi [9] and Hwang and Cheng [10] approached the problem treated by Mori and Uchida [8] using different numerical techniques. It is pointed out in [10] that Mori and Uchida's approximate analytical result for heat transfer based on Stuart's method starts deviation at $Ra = 3000$, from known numerical solutions [6, 7, 10], and about 25 per cent error is observed at Rayleigh number which is nine times the critical value of 1708.

The purpose of this paper is to study the effects of longitudinal vortex rolls in the post-critical regime on flow and heat transfer characteristics for fully developed laminar forced convection between two infinite horizontal parallel plates subjected to the uniform wall heat flux. The physical problem of interest here is the finite amplitude thermal convection in plane Poiseuille flow considering the nonlinear effect on the flow structure and temperature field. The present problem is characterized by the interaction between the free and forced convections. Furthermore, the free convection phenomenon represents the interaction between the stable upper layer and the unstable lower layer. Because of the uncertainty and the absence of accurate theory, the wave number for the post-critical regime in this study will be taken to be the one which is predicted by the linear stability analysis [1] for the primary mode. The photographic results shown in Fig. 1 reveal that the wave number does not appear to vary appreciably, at least in the post-critical regime near the critical value. In view of the fact that Stuart's method is a perturbation approach and leads to appreciable error at higher Rayleigh numbers, a numerical solution [10, 11] is employed for the present problem.

2. THEORETICAL ANALYSIS

Consider a steady fully developed laminar forced convection in a post-critical regime between two infinite horizontal plates subjected to a uniform axial wall temperature gradient. The subject of interest here is the study of flow and heat transfer characteristics after the longitudinal vortex rolls set in. It will be assumed that the Boussinesq approximations are valid and the wave number in the post-critical regime is taken to be the one predicted by the linear stability analysis [1].

The coordinate system is shown in Fig. 2. In order to investigate the flow structure and temperature field in the post-critical regime, perturbation quantities are superimposed on the basic flow quantities as,

$$U = U_b + u',\ V = v',\ W = w',\ T = T_b + \theta' \quad \text{and} \quad P = P_b + p' \quad (1)$$

where the basic flow quantities U_b, T_b and P_b satisfy the well-known equations for plane

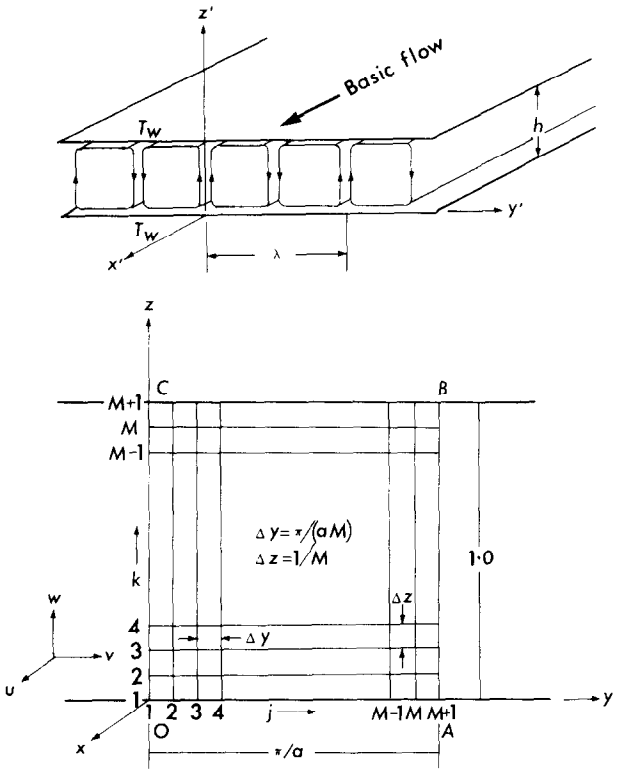

FIG. 2. Coordinate system and numerical grid.

Poiseuille flow. The solutions for the unperturbed state are:

$$\begin{aligned} U_b &= 4U_0(z - z^2) = U_0\phi_u/2 \\ T_b &= T_w - (U_0\tau h/\kappa)(z - 2z^3 + z^4)/3 \\ &= T_w - PrRe_0\,\tau h\,\phi_\theta \\ \phi_u &= 8(z - z^2) \\ \phi_\theta &= (2/3)(z - 2z^3 + z^4) \end{aligned} \tag{2}$$

where $z = z'/h$, U_0 is the maximum velocity in the unperturbed state, $\tau = \partial T/\partial x'$ is a constant axial temperature gradient and $Re_0 = U_0 h/(2\nu)$.

For the purpose of simplification and convenience, the following non-dimensional transformations and parameters are introduced.

$$(y', z') = (y, z)h, (u', v', w') = (Re_0\,u, v, w)\nu/h,$$
$$\theta' = PrRe_0\tau h\theta, \xi' = \xi\nu h^2, \psi' = \nu\psi,$$
$$\text{and } Gr = g\beta\tau h^4/\nu^2, Ra = PrGr. \tag{3}$$

By employing equations (1)–(3), the equations for the perturbation quantities can be obtained after some manipulation. The results are:

Axial momentum equation

$$v\frac{\partial u}{\partial y} + w\frac{\partial u}{\partial z} + w\frac{\partial \phi_u}{\partial z} = \nabla^2 u \tag{4}$$

Vorticity transport equation for secondary flow

$$v\frac{\partial \xi}{\partial y} + w\frac{\partial \xi}{\partial z} = \nabla^2\xi - Re_0 Ra\frac{\partial \theta}{\partial y} \tag{5}$$

where the dimensionless vorticity is

$$\xi = \nabla^2\psi \tag{6}$$

and the dimensionless stream function ψ is defined by

$$v = \partial\psi/\partial z,\ w = -\partial\psi/\partial y \tag{7}$$

Energy equation

$$u + Pr\left(v\frac{\partial\theta}{\partial y} + w\frac{\partial\theta}{\partial z} - w\frac{\partial\phi_\theta}{\partial z}\right) = \nabla^2\theta \tag{8}$$

where $\nabla^2 = \partial^2/\partial y^2 + \partial^2/\partial z^2$.

The boundary conditions are:

At the lower and upper plates,

$$u = \psi = \partial\psi/\partial z = \theta = 0.$$

Along the lines of symmetry $y = 0$, $0 < z < 1$ and $y = \pi/a, 0 < z < 1$, $\partial u/\partial y = \psi = \xi = \partial\theta/\partial y = 0$.

For the present problem, two parameters Pr and $Re_0 Ra$ appear in equations (4)–(8). In equation (4) one sees that the axial direction disturbance is caused mainly by the product of the vertical direction velocity disturbance, w, and the main flow velocity gradient $\partial\phi_u/\partial z$. This product is balanced by the remaining inertia terms, $v\,\partial u/\partial y$ and $w\partial u/\partial z$, and also by the viscous term $\nabla^2 u$. In equation (5), the secondary motion is seen to be driven by the unbalanced buoyant force term $Re_0 Ra\ \partial\theta/\partial y$. In the energy equation (8), the thermal disturbance is seen to come from two sources:

(a) the term due to the convective motion of the main flow disturbance, u,

(b) the term due to the vertical direction convection through the nonlinear basic temperature distribution, $Pr\,w\partial\phi_\theta/\partial z$.

For the case with small Prandtl number, the effect of source (a) is much more important than the effect of source (b). On the contrary, for the case with large Prandtl number, the effect of source (a) is negligible in comparison with the effect of source (b). Referring to equations (4)–(8) one notes that only a single parameter $PrRe_0Ra$ results for the case with large Prandtl number. When $Pr \to \infty$ and Re_0Ra is still very close to the critical value, the inertia terms, $v\,\partial\xi/\partial y$ and $w\,\partial\xi/\partial z$ in equation (5) and the term u representing the convective motion due to the main flow disturbance in equation (8) may be neglected as compared with the remaining terms in the respective equations. By transforming (v, w) into $(v, w)Re_0Ra$, only one parameter $PrRe_0Ra$ is left in the governing equations. This observation for large Prandtl number effect is also confirmed by the numerical results which will be presented later.

In view of the complexity of the equations (4)–(8) and the fact that an appreciable error is observed by applying Stuart's approximate method to the related problem [10] at higher Rayleigh numbers, the finite-difference technique is applied to the present problem. The detailed finite-difference approximations and the line iterative scheme will be omitted here for simplicity since they are reported elsewhere [10, 11].

Since the coefficient matrices for the finite-difference equations corresponding to the equations (4), (5) and (8) are not symmetric and their eigenvalues vary from step to step during the iteration of nonlinear terms, the determination of an optimal relaxation factor is very difficult. For most of the computations in the present problem, a relaxation factor of unity is used. An under-relaxation factor of 0·5 is often used to stabilize the numerical computation. The effect of grid size on the convergence of the flow and heat transfer results is also reported in [11]. For the present numerical solution, the number of divisions $M = 28$ is used to ensure the accuracy of the numerical result. It is noted that a prescribed error [10, 11] in the numerical computation is kept to be less than the order of 10^{-5}. The parameter $Re_0 = U_0h/(2\nu)$ can be converted readily to the parameter $Re = \bar{U}h/\nu$ which is based on the channel height and mean velocity by using the relation $Re = (4/3 + \bar{u})Re_0$.

3. RESULTS AND DISCUSSION

3.1 *Field characteristics for flow and temperature*

Before proceeding to the presentation of the overall flow and heat transfer results, it is instructive to examine the typical flow structure and temperature distributions in the post-critical regime in order to gain some insight into the heat transfer mechanism. The axial velocity distributions along three vertical lines for $Pr = 0{\cdot}7$ and $PrReRa = 30453$ are shown in Fig. 3 with comparison made against the

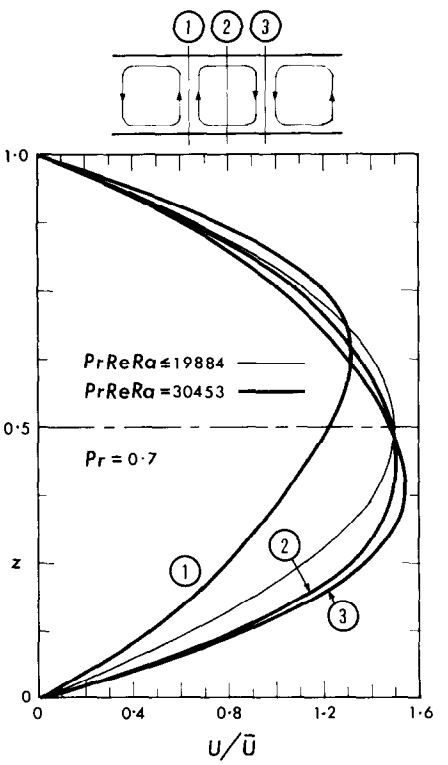

FIG. 3. Axial velocity distributions at $y = 0$, 0·868/2 and 0·868, together with Poiseuille profile.

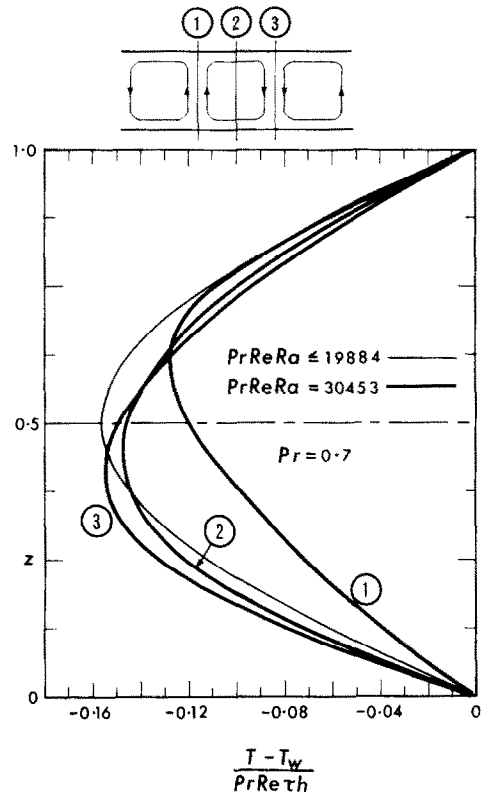

FIG. 4. Temperature distributions at $y = 0$, 0·868/2 and 0·868 together with profile from unperturbed flow.

plane Poiseuille flow velocity profile. It is seen that due to the secondary flow the axial velocity profile along section 1 is shifted upward and the axial velocity profiles along sections 2 and 3 are shifted downward. This also implies that the eye of the secondary motion is located somewhere between sections 1 and 2. Figure 3 also suggests that stronger secondary motion prevails in the lower half of the channel and particularly in the region near section 1.

The temperature distributions along three vertical lines for $Pr = 0{\cdot}7$ and $PrReRa = 30453$ are shown in Fig. 4 together with the temperature profile for the unperturbed state. As in the case of the axial velocity distributions, one is impressed with the distortion of the temperature profile from the basic profile in the lower half of the channel particularly in the region near section 1.

The distributions of the streamlines, constant vorticity lines and isotherms are shown in Figs. 5–7, respectively, for $Pr = 0{\cdot}7$ and $PrReRa = 30453$, 60000 and 73326. The three typical secondary flow streamlines illustrated in Fig. 5 show the gradual development of the stream line patterns and confirm that the intensity of the secondary motion is stronger in the lower half of the channel since the unstable region is

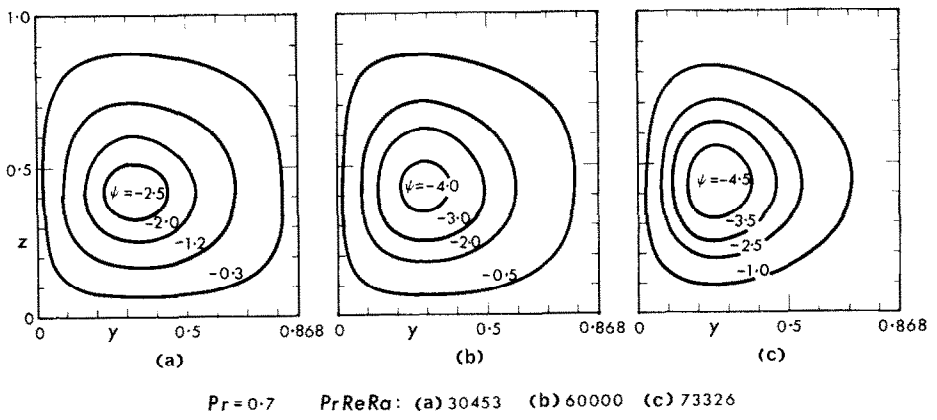

FIG. 5. Secondary flow streamlines for $Pr = 0{\cdot}7$ at three selected values of $PrReRa$.

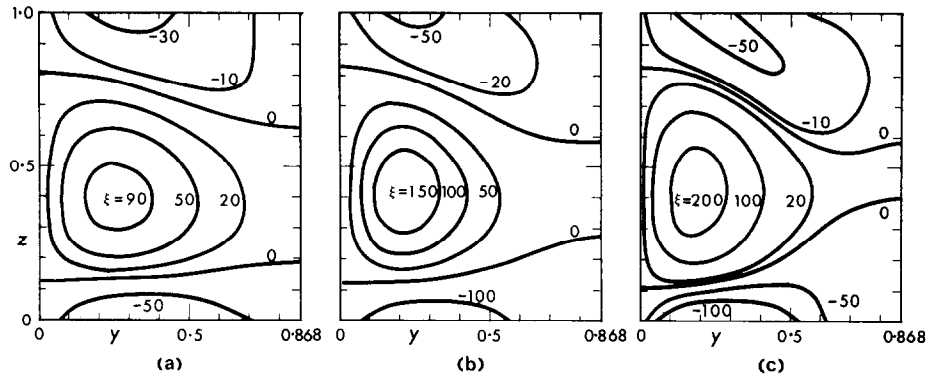

FIG. 6. Constant vorticity lines for $Pr = 0{\cdot}7$ at three selected values of $PrReRa$.

confined to that part of the channel only. By noting the location of the eye and the distributions of the streamlines, the relative intensity of the secondary motion throughout the region can be gained. The upward stream near $y = 0$ is much stronger than the downward stream near $y = 0{\cdot}868$. It is of interest to note that the secondary flow pattern presented in Fig 5(a) for $PrReRa = 30453$ can be compared with the experimental photograph shown in Fig. 1 for $Pr = 0{\cdot}7$ and $ReRa = 4{\cdot}65 \times 10^4$ ($PrReRa = 32600$).

For the unperturbed flow, the vorticity is zero everywhere. Figure 6 reveals that with secondary flow, two sources of vorticity with negative sign appear at the lower and upper plates. The strength of the vorticity source at the lower plate is seen to be stronger than the one at the upper plate. The vorticities generated at the lower and upper plates are dissipated into the central region as a sink of the vorticity with positive sign. As the value of the parameter $PrReRa$ increases, the strengths of the sources and sink increase correspondingly.

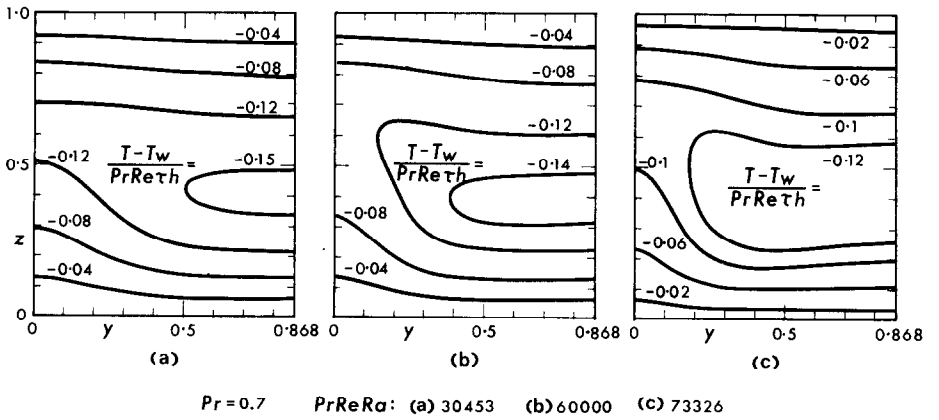

FIG. 7. Isotherms for $Pr = 0{\cdot}7$ at three selected values of $PrReRa$.

For the unperturbed flow, the isotherms are straight and parallel to the plates. With the secondary motion the isotherms become distorted as shown in Fig. 7. In response to the stronger secondary motion in the region $0 \leqslant y, z \leqslant 0{\cdot}5$, the isotherms are seen to be distorted considerably there than in the remaining region of the channel. As the value of the parameter $PrReRa$ increases, the distortion of the isotherms becomes progressively pronounced.

3.2 *Pressure-drop and heat transfer parameters*

In order to compute pressure drop and heat transfer rate in design, the values for the product of friction factor and Reynolds number (fRe) and the Nusselt number (Nu) are required. Following the usual definitions, the expressions for fRe and Nu can be written as follows:

$$(fRe)_1 = \frac{2 \cdot \left|4 + \frac{1}{2}\left(\frac{\partial \bar{u}}{\partial z}\right)_{z=0}\right|}{\left(\frac{2}{3} + \frac{\bar{u}}{2}\right)}, \text{ at lower plate} \quad (9)$$

$$(fRe)_2 = \frac{2 \cdot \left|-4 + \frac{1}{2}\left(\frac{\partial \bar{u}}{\partial z}\right)_{z=1}\right|}{\left(\frac{2}{3} + \frac{\bar{u}}{2}\right)}, \text{ at upper plate} \quad (10)$$

$$(fRe)_3 = [(fRe)_1 + (fRe)_2]/2 = 8/\left(\frac{2}{3} + \frac{\bar{u}}{2}\right),$$

from overall force balance (11)

where

$$f_1 = 2\mu\left|\frac{\partial \overline{U}}{\partial z'}\right|_{z'=0} / \rho \overline{U}^2, \quad f_2 = 2\mu\left|\frac{\partial \overline{U}}{\partial z'}\right|_{z'=h} / \rho \overline{U}^2,$$

$f_3 = (\partial P/\partial x')h/\rho \overline{U}^2$ and $Re = \overline{U}\, h/\nu$

$$(Nu)_1 = \frac{\left[\frac{2}{3} - \left(\frac{\partial \bar{\theta}}{\partial z}\right)_{z=0}\right]}{(\phi_\theta - \theta)_M}, \text{ at lower plate} \quad (12)$$

$$(Nu)_2 = \frac{\left[\frac{2}{3} - \left(\frac{\partial \bar{\theta}}{\partial z}\right)_{z=1}\right]}{(\phi_\theta - \theta)_M}, \text{ at upper plate} \quad (13)$$

$$(Nu)_3 = \frac{(Nu)_1 + (Nu)_2}{2} = \frac{2/3 + \bar{u}/2}{(\phi_\theta - \theta)_M},$$

from overall energy balance (14)

where

$$(\phi_\theta - \theta)_M = \int_0^1 \int_0^{\pi/a} (\phi_\theta - \theta)\, U \, dy \, dz/(\overline{U}\, \pi/a)$$

$$= \frac{T_w - T_M}{PrRe_0 \tau h}.$$

It is noted that all the average velocity and temperature gradients contained in the above definitions (9)–(14) are evaluated by using non-central five-point finite-difference formula and all the integrations are carried out by using Simpson's rule.

The flow result in the form of the ratio $(fRe)_i/(fRe)_0$ $(i = 1, 2, 3)$ vs. $PrReRa$ with Pr as a parameter is shown in Fig. 8. For a given finite value of $PrReRa$ with large Pr, the value of $ReRa$ is small and the intensity of the secondary motion is weak. Thus, the increment of the value for $(fRe)_3$ corresponding to the effect of the secondary motion on flow result is not significant. For example, Fig. 8 indicates that at $PrReRa = 2 \times 10^5$ (about eight times the critical value of $PrReRa$) the friction factor increases by about one per cent only for $Pr = 10$ as compared with the case without secondary flow. Thus, one can conclude that the effect of the secondary motion on flow result is significant only when the Prandtl number is small.

Figure 9 presents the results for Nusselt number ratio $(Nu)_i/(Nu)_0$ $(i = 1, 2, 3)$ vs. $PrReRa$ for various Prandtl numbers. It is recalled that the adoption of the product of Pr and $ReRa$ as a single parameter is based on the observation that an asymptotic behavior for heat transfer results exists as $Pr \to \infty$. For example, for a given value for $PrReRa = (PrReRa)^*$, the value of $(Nu)_3/(Nu)_0$ for $Pr \geqslant 2$ is seen to approach the asymptotic solution for $Pr \geqslant 10$ with a largest difference of about three per cent within the range of present

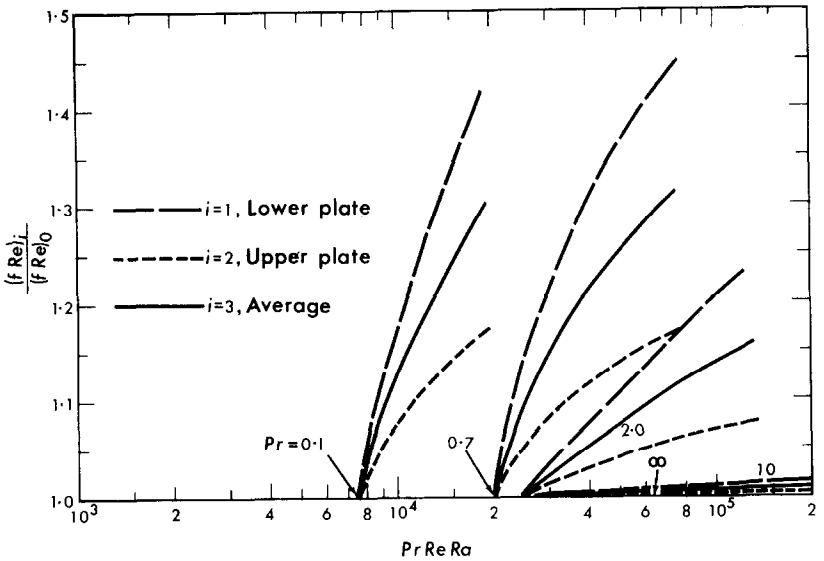

FIG. 8. Flow results for $Pr = 0{\cdot}1,\ 0{\cdot}7,\ 2,\ 10$ and ∞.

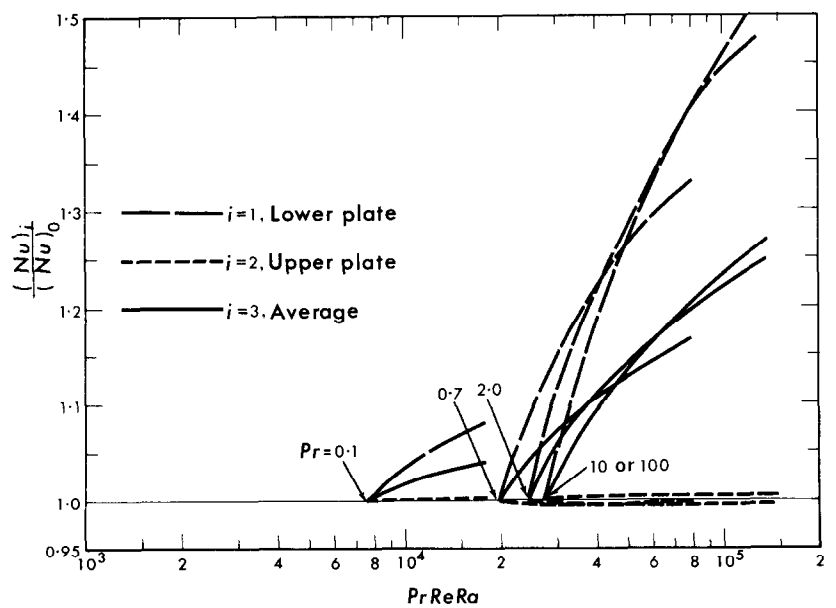

FIG. 9. Heat transfer results for $Pr = 0{\cdot}1,\ 0{\cdot}7,\ 2,\ 10$ and 100.

investigation. It is of interest to note that the value of $(Nu)_2/(Nu)_0$ is approximately one regardless of the value of Prandtl number. This is apparently due to the fact that the heat transfer rate at the upper plate is not affected by the rather weak secondary motion near the upper plate.

4. CONCLUDING REMARKS

1. It has been confirmed that the numerical solution using the boundary vorticity method [10, 11] is quite effective for the present rather complicated finite amplitude convection problem. The detailed convergence study for the numerical solution is given elsewhere [10, 11]. The method is expected to be valid for the numerical solution of finite amplitude convection due to body forces other than the buoyancy forces.

2. The numerical results reveal that for $Pr \geqslant 10$ the effect of secondary flow on the pressure-drop parameter fRe can be neglected. On the other hand, after reaching a critical value for $PrReRa$, the heat transfer results for $Pr = 2$ nearly coincides with the result for $Pr = 10$. This asymptotic behavior for the heat transfer result using a parameter $PrReRa$ suggests that one need not carry out the numerical computations for all the Prandtl numbers ranging from 2 to ∞ in order to study the Prandtl number effect. In this connection, one may mention that the possibility for a simple correlation for Prandtl number effect on forced convective heat transfer with secondary flow was pointed out in [12].

3. The assumption that the wave number in the post-critical regime does not deviate from the critical value determined by the linear stability analysis is believed to be a reasonable one based on the photographic results shown in Fig. 1. However, it is probable that the wave number in the post-critical regime is determined in the thermal entrance region instead of the fully developed region considered in this study. A study in the thermal entrance region might shed some light regarding the variation of the wave number in the post-critical regime.

4. The results of the present study clearly indicate that an advantage can be taken of the longitudinal vortex rolls to promote the heat transfer rate. In particular, it is significant to note that considerable improvement in heat transfer rate can be achieved with little increase in the friction factor for large Prandtl number fluids.

5. In applying the present results to a horizontal rectangular channel with a large aspect ratio, the free convection effect due to side walls must be examined. Some guidance in this respect can be provided by Fig. 1 and the experimental results reported in [2].

ACKNOWLEDGEMENTS

The authors are indebted to Professor E. M. Sparrow of The University of Minnesota who, as an external examiner for the final Ph.D. thesis examination of G. J. Hwang, pointed out the desirability of using the mean axial velocity $\bar{U}$ instead of the maximum axial velocity U_0 in the unperturbed state for presenting flow and heat transfer results. The authors also wish to thank Mr. M. Akiyama for his cooperation in obtaining Fig. 1, and Mrs. Evelyn Buchanan for typing the manuscript.

REFERENCES

1. W. NAKAYAMA, G. J. HWANG and K. C. CHENG. Thermal instability in plane Poiseuille flow. *J. Heat Transfer* **92**, 61–68 (1970).
2. M. AKIYAMA, G. J. HWANG and K. C. CHENG. Experiments on the onset of longitudinal vortices in laminar forced convection between horizontal plates. *J. Heat Transfer*, **93**, 335–341 (1971).
3. W. V. R. MALKUS and G. VERONIS. Finite amplitude cellular convection. *J. Fluid Mech.* **4**, 225–260 (1958).
4. J. T. STUART. On the non-linear mechanics of hydrodynamic stability. *J. Fluid Mech.* **4**, 1–21 (1958).
5. P. H. ROBERTS. On nonlinear Bénard convection. *Non-Equilibrium Thermodynamics. Variational Techniques and Stability*, edited by R. J. DONNELLY, R. HERMAN and I. PRIGOGINE. The University of Chicago Press, Chicago and London (1966).
6. J. E. FROMM. Numerical solutions of the nonlinear equations for a heated fluid layer. *Physics Fluids* **8**, 1757–1774 (1965).
7. W. H. PLOWS. Some numerical results for two-dimensional steady laminar Bénard convection. *Physics Fluids* **11**, 1593–1599 (1968).
8. Y. MORI and Y. UCHIDA. Forced convective heat

transfer between horizontal flat plates. *Int. J. Heat Mass Transfer* **9**, 803–817 (1966).
9. Y. OGURA and A. YAGIHASHI, A numerical study of convection rolls in a flow between horizontal parallel plates. *J. Met. Soc. Japan* **47**, 205–217 (1969).
10. G. J. HWANG and K. C. CHENG. A boundary vorticity method for finite amplitude convection in plane Poiseuille flow. Proc. 12th Midwestern Mechanics Conference. University of Notre Dame (1971).
11. G. J. HWANG. Thermal instability and finite amplitude convection with secondary flow. Ph.D. Thesis. University of Alberta, Edmonton, Alberta, Canada (1970).
12. K. C. CHENG. G. J. HWANG and M. AKIYAMA. On a simple correlation for Prandtl number effect on forced convective heat transfer with secondary flow. To be published in *Int. J. Heat Mass Transfer*.

CONVECTION À AMPLITUDE FINIE AVEC DES TOURBILLONS LONGITUDINAUX DANS L'ÉCOULEMENT PLAN DE POISEUILLE. EFFET DU GRADIENT DE TEMPÉRATURE AXIAL UNIFORME

Résumé—Une convection à amplitude finie avec des rouleaux tourbillonnaires longitudinaux pour un écoulement permanent laminaire forcé entièrement développé hydrodynamiquement et thermiquement entre deux plaques planes horizontales et infinies soumises à un flux thermique pariétal uniforme longitudinalement a été étudiée par une résolution aux différences finies qui utilise une combinaison de la méthode de vorticité limite et d'une technique de relaxation linéaire itérative. Les équations écrites avec les approximations de Boussinesq ont été résolues jusqu'à quatre fois la valeur critique du paramètre $PrReRa$. L'établissement de l'écoulement secondaire sous forme de rouleaux tourbillonnaires longitudinaux est associé à une valeur critique $PrReRa$ qui peut être obtenue par une analyse de stabilité linéaire avec perturbation infinitésimale. On suppose que le nombre d'onde dans le régime post-critique d'écoulement est celui calculé dans l'analyse de stabilité linéaire. Le mécanisme de transfert thermique est clarifié par une étude détaillée faite pour des écoulements et des températures relatifs à l'air ($Pr = 0{,}7$). On présente aussi une série de photographies décrivant le développement graduel des rouleaux tourbillonnaires longitudinaux pour l'air. On donne les résultats de l'écoulement et du transfert thermique pour $Pr = 0{,}1$; 0,7; 2; 10 et 100. Une étude de l'influence du nombre de Prandtl révèle que l'effet de l'écoulement secondaire sur le paramètre de perte de pression fRe peut être négligé pour $Pr = 10$ et qu'un comportement asymptotique des résultats du transfert thermique existe pour $Pr = 2$ dans le régime post-critique.

KONVEKTION ENDLICHER AMPLITUDE MIT LÄNGSWIRBEL IN EBENER POISEUILLE-STRÖMUNG—DER EINFLUSS EINES GLEICHMÄSSIGEN AXIALEN TEMPERATURGRADIENTEN

Zusammenfassung—Die Konvektion bei endlicher Amplitude mit longitudinalen Wirbelrollen in einer stationären, hydrodynamisch und thermisch eingelaufenen laminaren Strömung zwischen zwei unendlichen, waagrechten und ebenen Platten, die gleichmässige Wärmestromdichte liefern, wurde mit einem endlichen Differenzenverfahren zu lösen versucht. Dabei wurde die Kombination einer Grenzschicht-Wirbelmethode und einer iterativen Relaxationsmethode verwendet. Die bestimmenden Gleichungen mit den Näherungen von Boussinesqu werden bis zum 4-fachen des kritischen Wertes des Parameters ($Pr \cdot Re \cdot Ra$) gelöst. Der Beginn der Sekundärströmung in Form von längsgestreckten Wirbelrollen wird durch einen kritischen Wert von $(PrReRa)^*$ angezeigt, der errechnet werden kann mit Hilfe der linearen Stabilitätsanalyse bei unendlich kleinen Störungen. Als Wellenzahl im überkritischen Strömungsgebiet wird die sich aus der linearen Stabilitätsanalyse ergebende angenommen.

Die Art des Wärmeübergangs wird durch eine eingehende Untersuchung des Strömungs- und Temperaturfeldes bei Luft ($Pr = 0{,}7$) geklärt. Eine Serie von photographischen Aufnahmen wird gezeigt, die eine allmähliche Entwicklung der längsgestreckten Wirbelrollen darstellen. Die Ergebnisse der Strömung und des Wärmeüberganges werden für $Pr = 0{,}1$, 0,7, 2, 10 und 100 wiedergegeben.

Die Untersuchung über den Einfluss der Prandtl-Zahl zeigt, dass die Auswirkung der Sekundärströmung auf den Druckabfallparameter $f(Re)$ vernachlässigt werden kann bei $Pr = 10$. Für $Pr = 2$ liegt ein asymptotisches Verhalten der Wärmeübergangsergebnisse im überkritischen Gebiet vor.

КОНВЕКЦИЯ КОНЕЧНОЙ АМПЛИТУДЫ С ПРОДОЛЬНЫМИ ЗАВИХРЕНИЯМИ В ПЛОСКОМ ПУАЗЕЙЛЕВСКОМ ТЕЧЕНИИ. ВЛИЯНИЕ РАВНОМЕРНОГО АКСИАЛЬНОГО ГРАДИЕНТА ТЕМПЕРАТУРЫ

Аннотация—Задача о конвекции с конечной амплитудой с продольными вихревыми валами в устойчивом гидродинамически и термически полностью развитом ламинарном вынужденном течении между двумя бесконечными плоскими пластинами при аксиальном однородном тепловом потоке на стенке решается приближенно методом конечных разностей и спомощью итерационного процесса с использованием релаксации и граничных условий для завихренности. Основные уравнения в приближении Буссинеска решаются до значения параметра ($Pr\ Re\ Ra$), в четыре раза превышающею критическое. На возникновение вторичного течения в форме продольных вихревых валов указывает критическое значение ($Pr\ Re\ Ra$)*, которое может быть получено из анализа линейной устойчивости. Механизм теплообмена выясняется из детального исследования характеристик полей скорости и температуры на примере воздуха ($Pr = 0{,}7$). Представлена серия фотографий, изображающих постепенное развитие продольных вихревых валов для воздуха. Представлены результаты по гидродинамике и теплообмену для $Pr = 0{,}1$; 0,7 ; 10 и 100. Исследование влияния числа Прандтля показывает, что влиянием вторичного течения на параметр перепада давления $f\ Re$ можно пренебречь для $Pr = 10$, а асимптотическое поведение коэффициентов теплообмена обнаружено для $Pr = 2$ в закритическом режиме.